Solid-State Electronics 88 (2013) 89–94

Contents lists available at SciVerse ScienceDirect

Solid-State Electronics

journal homepage: www.elsevier.com/locate/sse

Pressure sensors based on suspended graphene membranes

Anderson.D. Smith [a], Sam Vaziri [a], Frank Niklaus [a], Andreas.C. Fischer [a], Mikael Sterner [a], Anna Delin [a], Mikael Östling [a], Max.C. Lemme [a,b,*]

[a] KTH Royal Institute of Technology, Electrum 229, 16440 Kista, Sweden
[b] University of Siegen, Hölderlinstr. 3, 57076 Siegen, Germany

ARTICLE INFO

Article history:
Available online 2 June 2013

Keywords:
Graphene
Sensor
Pressure
Nanotechnology
NEMS and Nanoelectromechanical System
Piezoresistive

ABSTRACT

A novel pressure sensor based on a suspended graphene membrane is proposed. The sensing mechanism is explained based on tight binding calculations of strain-induced changes in the band structure. A CMOS compatible fabrication process is proposed and used to fabricate prototypes. Electrical measurement data demonstrates the feasibility of the approach, which has the advantage of not requiring a separate strain gauge, i.e. the strain gauge is integral part of the pressure sensor membrane. Hence, graphene membrane based pressure sensors can in principle be scaled quite aggressively in size.

1. Introduction

Graphene, experimentally discovered in 2004 [1,2], shows a number of exceptional properties which make it a very promising material for electronic devices. Some of its notable properties include a high carrier mobility of up to 200,000 $cm^2/V\,s$ for suspended graphene membranes [3,4], as well as a high velocity saturation of 3×10^7 cm/s [5]. Graphene's extraordinary characteristics can be explained with its electronic band structure. Around each of the k-points, one can observe a linear dispersion relation, a consequence of the two-dimensional honeycomb structure of carbon atoms in graphene with two atoms in the primitive unit cell. Further, graphene has no band gap ($E_g \approx 0$ eV). While the linear dispersion relation leads to a very low effective mass of both electrons and holes, and hence high carrier mobility, the absence of a band gap severely limits the applicability for logic devices [6]. When graphene is strained, however, the electronic structure changes, and simulations have predicted band gaps in highly strained graphene of up to 0.95 eV [7–10]. Along these lines, it was shown experimentally that the resistivity of graphene changes when it is strained [11]. In addition to its remarkable electronic properties, graphene also shows extraordinary mechanical properties. The Young's modulus for graphene has been found to be roughly $E = 1.0$ TP [12], which makes it the strongest material known today. Graphene is also stretchable by at least 20% [13].

The unique combination of electronic and mechanical properties makes graphene an ideal material for sensor applications involving electromechanical coupling, particularly since its mono-atomic thickness adds to its merits: In micromachined pressure sensors, the sensitivity of a device strongly correlates with the membrane thickness and the transduction (strain sensing) mechanism in the pressure senor membrane [14]. I.e. the thinner the pressure sensor membrane, the smaller it can be made for a given strain measurement sensitivity. In this paper, we propose a device structure and a fabrication method for graphene membrane based pressure sensors and demonstrate electromechanical coupling in suspended graphene membranes. In this concept, nanoelectromechanical system (NEMS), place a graphene membrane over a cavity etched into a silicon dioxide (SiO_2) film. When placed inside a vacuum environment, the pressure difference between air inside the cavity and the vacuum on the outside of the cavity causes the graphene membrane to deflect, thus straining it proportional to the chamber pressure. The piezoresistive effect should lead to change in resistance as a function of pressure. A schematic of the mechanism is shown in Fig. 1. The concept utilizes the extraordinary stiffness of graphene membranes [15], the strong adhesion of graphene to SiO_2 [16] and the fact that graphene membranes are impermeable, even for helium [17]. The structure of the proposed device, including electrical contacts is shown in Fig. 2a and b. The resistance of the graphene as a function of pressure is evaluated by four-probe resistance measurements using the four contacts of the device structure.

2. Simulation

Various models predict band gaps in strained graphene of up to $E_g = 0.95$ eV [7–9]. The magnitude of the band gap depends strongly on the strain orientation, i.e. whether uniaxial zig-zag or

---

[*] Corresponding author at: KTH Royal Institute of Technology, Electrum 229, 16440 Kista, Sweden. Tel.: +46 8 790 4351.
E-mail address: lemme@kth.se (Max.C. Lemme).

0038-1101/$ - see front matter © 2013 Elsevier Ltd. All rights reserved.
http://dx.doi.org/10.1016/j.sse.2013.04.019

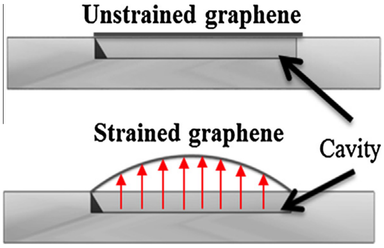

Fig. 1. (a) Schematic of an unstrained graphene layer over a cavity. (b) Schematic of a strained graphene membrane. The red arrows indicate the force exerted by a pressure difference between the vacuum chamber and the air inside the cavity. (For interpretation of the references to color in this figure legend, the reader is referred to the web version of this article.)

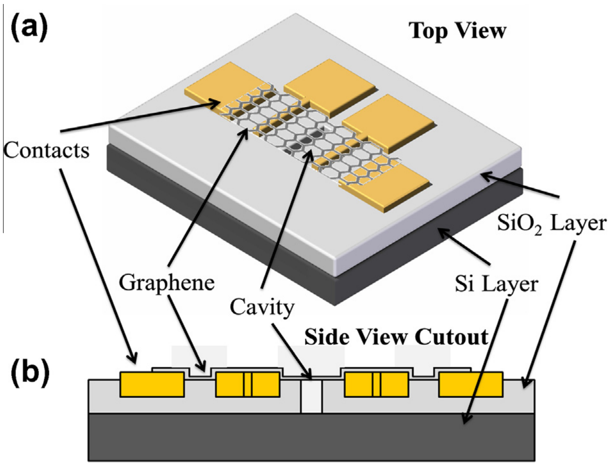

Fig. 2. (a) Isometric view of the proposed device structure. (b) Cross sectional view of the proposed device structure.

armchair strain, shear strain, or combinations thereof are calculated. In this work, we used a tight-binding model after Cocco et al. [9]. Fig. 3a shows the band structure of graphene for an unstrained case and Fig. 3b shows a strained case of 23% in the armchair direction. We specifically chose 23% strain in the armchair direction in order to verify our model against previous literature data, which shows band gap openings at 23% strain [9]. Our model uses the potential scaling function of Xu et al. [18], which was calibrated to match interatomic distances for graphene [17]. While this is a rough simplification, it generally approximates where band gap opening occurs in the armchair direction. While such strain levels and large band gaps are beyond the values achievable in our experiment, the key is that the band structure changes when graphene is strained. Fig. 3c shows the density of states (DOS) corresponding to the extreme cases of 0% and 23 % strain. This change in DOS is important because a change in DOS will directly impact the conductance of the material and thereby impact its resistance. While the model does not provide a direct correlation between Fermi level and strain (or strain and resistance) at this point, it can be said qualitatively that a shift in the DOS level occurs due to a change in the strain. This is because strain moves the location of the Fermi crossing away from the high-symmetry points even for small strain [19]. Fig. 4a also shows a corresponding top view of the band structure that illustrates the shift in the location of the Dirac points. These shifts in band structure and DOS are present regardless of the strain direction, which means that they will occur regardless of the orientation of the graphene with respect to the cavity and the contacts.

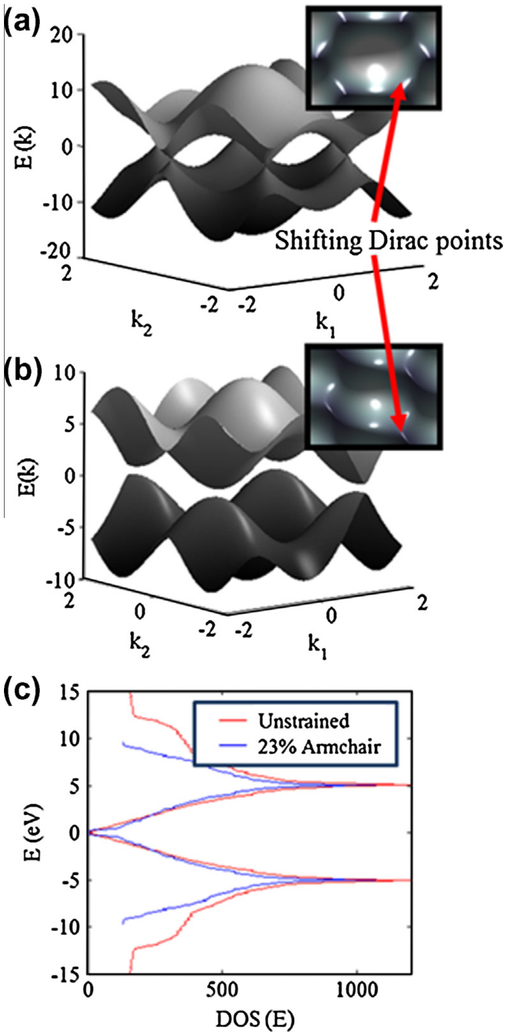

Fig. 3. (a) Calculated band structure of unstrained graphene. Insert: top view. (b) Calculated band structure for graphene with 23% armchair strain. Insert: top view. (c) Density of states (DOS) for unstrained and 23% strained graphene.

3. Experimental

3.1. Device fabrication

Devices were fabricated on thermally oxidized silicon chips with a SiO_2 thickness of 2 µm. First, cavities were defined with photoresist and etched 1.5 µm deep into the SiO_2 layer with a reactive ion etching process using Ar and CHF_3 at 200 mW and 40 mTorr. Then, 640 nm deep cavities were defined and etched into the substrate for the contact layers. 160 nm of Ti and 500 nm of Au were deposited into the contact cavities in a self-aligned process. After lift-off, the Au rises over the surface of the substrate by 20 nm. These predefined contacts were chosen to minimize processing of the chips after graphene transfer. Next, single layer CVD graphene grown on copper was transferred onto the chips. To this end, poly methyl methacrylate (PMMA) was spun onto the graphene as a carrier layer. The graphene on the backside of the foil was etched using O_2 plasma. The copper was then wet etched using ferric chloride leaving the graphene on PMMA floating in the liquid. These steps are illustrated in Fig. 4a. The graphene was then transferred and rinsed in de-ionized water and picked up with the chip. The chip was baked for 5 min at 45 °C in order to dry it and let the graphene adhere to the substrate. The chip fabrication steps and the final graphene transfer are illustrated in Fig. 4b. Next,